Materials Science Forum Vols. 636-637 (2010) pp 338-343

doi:10.4028/www.scientific.net/MSF.636-637.338

Influence of Oxygen Stoichiometry and Cation Ordering on Magnetoresistive Properties of $Sr_2FeMoO_{6\pm\delta}$

M. Kalanda[1,a], G. Suchaneck[2,b], A. Saad[3,c], S. Demyanov[1] and G. Gerlach[2]

[1]Scientific-Practical Materials Research Centre, NAS of Belarus, 220072 Minsk, Belarus

[2]TU Dresden, Solid State Electronics Lab, 01062 Dresden, Germany

[3]Al-Balqa Applied University, 19117 Salt, Jordan

[a]kalanda@ifttp.bas-net.by, [b]Gunnar.Suchaneck@tu-dresden.de, [c]daas005@yahoo.co.uk

Keywords: Spintronics, Double perovskite, Oxygen stoichiometry, Magnetization, Superstructural ordering

Abstract. This work investigates the influence of initial compound synthesis prehistory on the phase sequence during formation of single-phase $Sr_2FeMoO_{6\pm\delta}$ (SFMO). Analytical-grade $SrCO_3$, Fe_2O_3 and MoO_3 (sample No.1) and partially reduced precursors of $SrFeO_{3-x}$ (SFO) and $SrMoO_{4-y}$ (SMO) (sample No.2) were used as initial reagents. In the latter case, kinetic limitations of SFMO phase formation are resolved by increasing the diffusivity of both of Fe^{3+} and Mo^{5+} and decreasing diffusion lengths to the reaction zone. This enhances the double-perovskite growth rate, lowers synthesis temperature and increases the intensity of X-ray reflections of (011) and (013) planes suggesting a superstructural ordering of Fe^{3+} and Mo^{5+} cations. Samples No.1 and No.2 have both a $T_c \sim 420$K while the magnetization value at 77 K in the sample No.2 is higher by a factor 2.3 compared to that of sample No.1. A decrease of the oxygen vacancy concentration by annealing $Sr_2FeMoO_{5.82}$ lowered magnetization of the samples and promoted the formation of a second magnetic phase with $T_c = 700$ K. We suppose that an increase of oxygen partial pressure during annealing causes formation of clusters with antiferromagnetic coupling in Fe^{3+}-O^{2-}-Fe^{3+} chains. In order to increase the magnetoresistive effect at temperatures relevant for technical application, weak intergrain bonds should be formed.

Introduction

Magnetic half-metallic systems $Sr_2FeMoO_{6-\delta}$ (SFMO) with ordered double perovskite structure are promising materials for spintronic devices. SFMO has a high Curie temperature of 420 K [1], a high low-field magnetic resistance (MR) associated with grain boundary tunnelling [2], and an about entire spin polarization [3]. Upon cooling of SFMO powder samples, a phase transition of the type $Fm\bar{3}m \rightarrow I4/m$ was obtained at about 400 K by neutron diffraction [3, 4]. In the tetragonal $I4/m$ structure, the FeO_6 and MoO_6 octahedra rotate continuously around the c-axis. Electron spins of Fe and Mo atoms are arranged in ferromagnetic Fe/Mo planes that are mutually intersected at an angle of 120°. A ferromagnetic structure with partial compensation of Fe and Mo cation magnetic moments is formed due to an antiparallel spin alignment in the double perovskite crystal lattice [5,6]. The ferrimagnetic structure of the complex oxide reveals a half-metallic state with a predicted saturation moment of $4\mu_B$ at $T = 0$ K which is described by an antiferromagnetic coupling between the spins of Fe^{3+} ($3d^5$, S = 5/2) and Mo^{5+} ($4d^1$, S = 1/2) cations. Magnetic moments determined experimentally are systematically lower than the theoretical ones [5, 8-10] because of changes of antisite defects of the type Fe_{Mo} and Mo_{Fe}, changes in cation composition, appearance of magnetic clusters which modify the orientation of strongly hydridized Fe^{3+} and Mo^{5+} cation orbitals, etc.

Formation of the described structure defects depends predominantly on the oxygen stoichiometry index $6\pm\delta$ [11]. Therefore, processing conditions of the double perovskites should provide a correct oxygen partial pressure (p_{O2}) at a given temperature T. For instance, annealing in reducing atmosphere of Ar + 1 % H_2 at 1470 K is required to achieve a value of $6-\delta = 5.8$ [11]. Weak

intergrain bonds form nanojunctions and induce the effect of tunnelling magnetoresistance due to quantization of the spin-polarized current and the exchange splitting of conducting electrons. This results in controlling the conductivity by applying an external magnetic field. Thus, an optimization of double perovskite processing is required to control oxygen stoichiometry, concentration of Fe_{Mo} and Mo_{Fe} point defects, cation ordering, and also the presence of magnetically ordered clusters. The search for different routes of SFMO fabrication is attributed to the complex phase transitions and to the slow SFMO formation because of low Fe^{3+} and Mo^{5+} mobilities [12, 13].

This work investigates the influence of the sample prehistory, i.e., the initial compound synthesis, on the rate of SFMO phase formation and cation ordering in the crystal structure where magnetic properties of SFMO are critically dependent on the cation disorder and on the value of oxygen stoichiometry index.

Experimental

In order to investigate the influence of the starting compounds on the phase transitions during $Sr_2FeMoO_{6\pm\delta}$ (SFMO) crystallization, analytical-grade $SrCO_3$, Fe_2O_3 and MoO_3 (sample No.1) and partially reduced precursors of $SrFeO_{3-x}$ (SFO) and $SrMoO_{4-y}$ (SMO) (sample No.2) were used for synthesis. Complex oxides were also manufactured by conventional ceramic processing from oxides of MoO_3 and Fe_2O_3, and strontium carbonate, $SrCO_3$. Mixing the components in stoichiometric ratio and milling were conducted in alcohol using a vibromill for 3 hours. The resulting mixture was dried at 350 K and pressed into tablets (diameter = 10 mm, thickness = 4…5 mm) at 3 GPa (MoO_3, Fe_2O_3 and $SrCO_3$) and at 86 GPa (SFO and SMO), respectively. For SFO and SMO precursor synthesis, preliminary annealing was performed in air for 20 to 40 hours at 970 K and at 1070 K for the same period, respectively. A second milling was conducted to increase sample homogeneity. The final synthesis was obtained in air for 20 to 40 hours at 1240 K (SFO) and 1270 K (SMO) with subsequent cooling with an initial rate of 200 K/min. Temperature control within ±0.5 K was performed by a RIF-101 regulator with a Pt-Pt/Rh thermocouple. Nanosized precursors ($d \sim 200$ nm) were finally fabricated by long-term (24 h) vibromilling in alcohol. The investigation of phase transitions during crystallization of SFMO was made for the samples annealed by dynamic heating in the temperature range between 300 and 1420 K with a rate of 120 K/h and a consequent quenching at room temperature. Sample annealing was performed in vacuum-sealed quartz ampoules consisting of an iron getter to provide reducing conditions.

X-ray diffraction pattern of the products of solid state synthesis was recorded with a scanning speed of 60°/h in the range $2\Theta = 10…90°$ using CuK_α radiation of a DRON-3 setup. Phase analysis was carried out by means of the ICSD-PDF2-2000 database using the software tools FULLPROF and POWDERCELL. The conversion degree α, i.e., the fraction of matter reacted into SFMO, was evaluated by means of the changes of the normalized diffraction peak intensities $[I_{211}(112)/\{I_{211}(112)+I_{101}(112)\}]\times100\%$, where $I_{211}(112)$ and $I_{101}(112)$ are the diffraction peaks with maximum intensity of SFMO and SMO, respectively. Tetragonal *P4/mmm* symmetry was considered. Magnetic and magnetoresistive properties of the samples were evaluated using a magnetometer with a magnetic field of up to 12 T directed along the electric current.

Magnetoresistance was determined as $MR = [R(B)-R(0)]/R(B)$, where $R(B)$ and $R(0)$ are the resistance values with and without magnetic field, respectively.

Results and Discussion

The following sequence of phase transitions was obtained by XRD during solid state synthesis from MoO_3, Fe_2O_3 and $SrCO_3$ in stoichiometric ratio as described above: {Fe_2O_3, MoO_3, $SrCO_3$} (300K) → {SMO, Fe_2O_3, $SrCO_3$} (770K) → {SMO, SFO(traces)), SFMO} (970K) → {SMO(traces), SFMO} (1170K) → {SFMO} (1420K) . Initially SMO was formed at about 770 K, while XRD peaks of SFO and SFMO appeared simultaneously at about 970K. As temperature increased, SFO

diffraction peaks disappeared in the temperature region between 970 and 1170 K while that of SMO remained up to 1370 K.

Formation of the SFMO initially includes the creation of SFO and SMO precursors which were employed also as initial components of solid state synthesis. This way prevented the intermediate formation and SFMO nucleation and growth were enhanced due to decreasing cation diffusion lengths to the reaction zone. XRD analysis of quenched samples synthesized as described above from SFO and SMO in stoichiometric ratio and pressed as tablets revealed the following sequence of phase transitions: {SMO, SFO} (770K) →{SMO, SFO, SFMO} (870K) → (SMO, SFO(traces); SFMO) (1170K) → {SMO(traces), SFMO} (1270K) → {SFMO} (1370K) (Fig. 1). The temperature of SMO impurity phase dissolution was decreased by 50 K as well as the intensity of SFO diffraction peaks when the tablets were pressed at high pressure increasing their density. This suggests that the limiting process in SFMO crystallization is volume diffusion through the product layer.

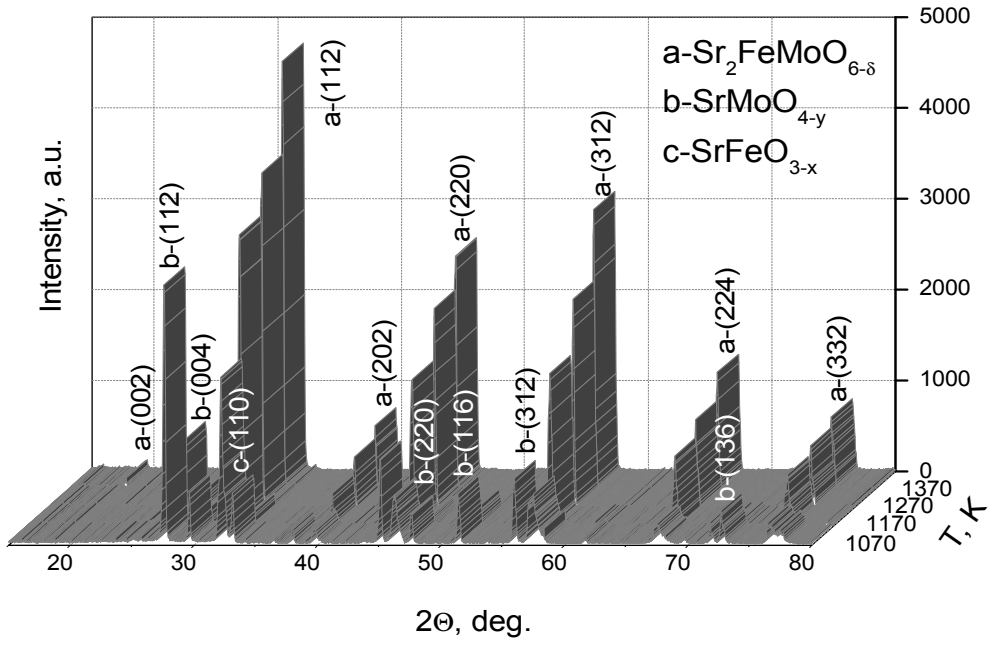

Fig. 1. XRD pattern of samples synthesized from SFO and SMO precursors.

SFO diffraction peaks shift to lower angles with increasing temperature in the range from 770 to 970 K (Fig. 2). This was attributed to the dissolution of a part of Mo^{5+} cations in the SFO crystal lattice resulting in volume increase. Moreover, SFO exhibits a large homogeneity region, 2.5 < 3-x < 3.0, within which three crystal modifications can exist: orthorhombic (2.5-2.75), tetragonal (2.75-2.87) and cubic (2.87-3) [14]. The obtained shift by 1…2° for the presented work is probably due to oxygen vacancies and the increase of unit cell volume. The temperature dependence of the conversion degree $\alpha = I_{211}(112)/\{\{I_{211}(112) + I_{101}(112)\}\}\cdot 100\%$ revealed two stages of SFMO growth (Fig. 3). The first stage is presumably limited by component interaction at phase boundaries while the second-stage reaction rate is limited by volume diffusion through the product layer. The transformation is determined by process period. For both stages the SFMO growth rate was higher for sample No.2. Using SFO and SMO precursors and high pressure for ceramic tablet fabrication, density and reactivity were increased but the mean diffusion length in the reaction zone decreased. Simultaneously, the number of reacting species was increased. On the other hand, oxygen deficiency in SFO favors anion diffusivity resulting in increase of the SFMO growth rate, the decrease of the crystallization temperature and the appearance of additional (101) and (103) XRD peaks suggesting Fe^{3+} and Mo^{5+} superstructure ordering (Fig. 4).

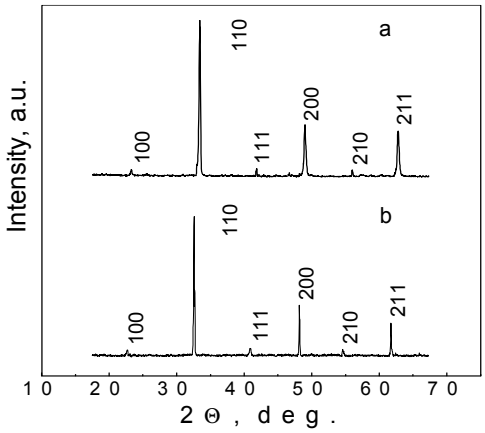

Fig. 2. XRD pattern of SFO samples. Quenching temperature 770 K (a), 970 K (b).

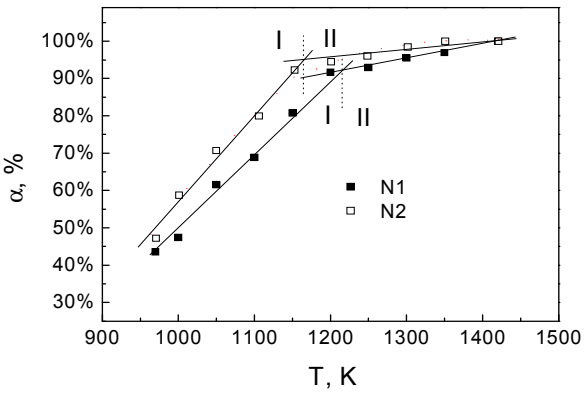

Fig. 3. Temperature dependence of the conversion degree into SFMO in quenched samples No.1 and No.2.

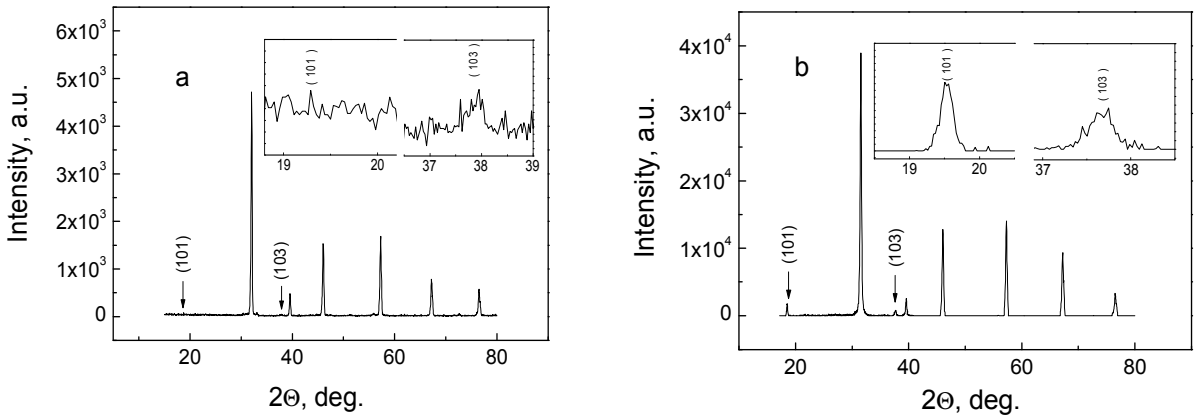

Fig. 4. XRD pattern of SFMO samples synthesized from a mixture of MoO_3, Fe_2O_3, and $SrCO_3$ (a) and from SFO and SMO precursors (b).

Figure 5 shows the temperature dependence of magnetization. A Curie temperature of 418 K was obtained both for sample No.1 and sample No.2. The magnetization per formula unit (f.u.) at 77 K amounts to $M_S = 1.33\mu_B$/f.u. for sample No.1 and $3.07\mu_B$/f.u. for sample No.2. Magnetization in the cation disordered sample No.1 is only 44% of the value of the dense sample No.2 exhibiting superstructure ordering (Fig. 5). The magnetic moment of double perovskite SFMO is determined by the antiparallel order of magnetic moments of $Fe^{3+}(3d^5)$ and $Mo^{5+}(4d^1)$ ions forming bonds of the Fe^{3+}-O-Mo^{5+} type. Therefore, the lower value caused by disordering of Fe and Mo ions (Fig. 4a) can be assigned also to antiferromagnetically coupled clusters of the type Fe^{3+}-O^{2-}-Fe^{3+} and Mo^{5+}-O^{2-}-Mo^{5+} [10]. The presence of magnetic clusters is evidenced indirectly from magnetoresistance measurements (Fig. 6). Maximum *MR* value for the two samples was $MR = 29\%$ at $T = 4.2$ K and $B = 8$ T for sample No.1 exhibiting a complex conductivity behaviour in the region of $B = 0...8$ T (Fig. 7). Similar magnetic clusters with an averaged radius of 20~30 nm were obtained by small-angle neutron scattering (SANS) in [15]. Decreasing oxygen vacancy concentration and increasing concentration of antisite defects Fe_{Mo} by annealing $Sr_2FeMoO_{5.82}$ at $p_{O2} = 10^4$ to 10^6 Pa lowered magnetization of the samples and promoted the formation of a second magnetic phase with $T_c = 700$ K (Fig. 8). According to the X-ray diffraction data, SMO phase appearance was observed which should cause an increase of Fe atoms content in SFMO. Subsequent annealing of multiple phase samples (SFMO, SMO) at 1423 K and $p_{O2} = 10^{-8}$ Pa for 50 h recovered the physical properties completely and made the samples single-phase. Fe atom precipitation on grain boundaries was

unlikely to occur in this case, because the increase of oxygen pressure during annealing should result in an increase of the amount of precipitated Fe atoms and, correspondingly, in an increase of the magnetic moment of the high-temperature magnetic phase with T_c = 700 K.

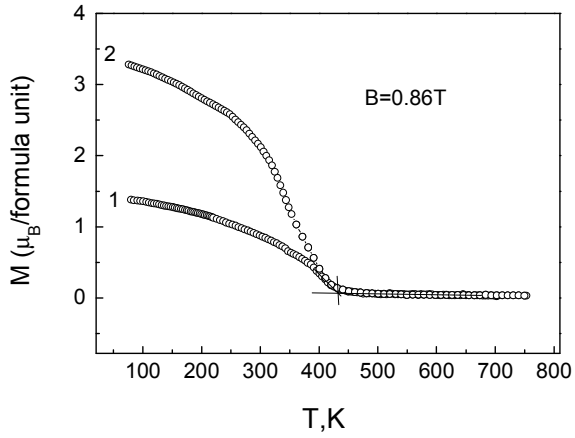

Fig. 5. Temperature dependence of magnetization of samples synthesized from a mixture of MoO_3, Fe_2O_3, and $SrCO_3$ (1), and from SFO and SMO precursors (2).

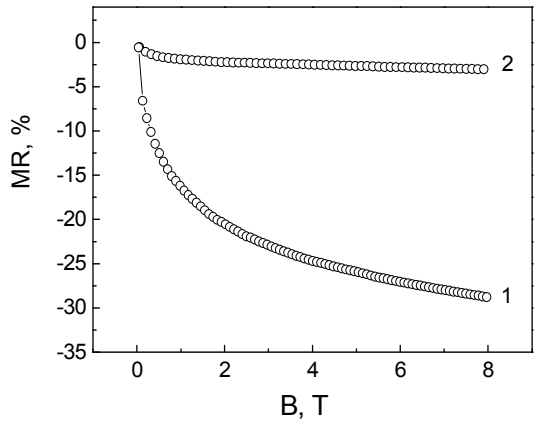

Fig. 6. Field dependence of magnetoresistive effect in samples No.1 and No.2 .

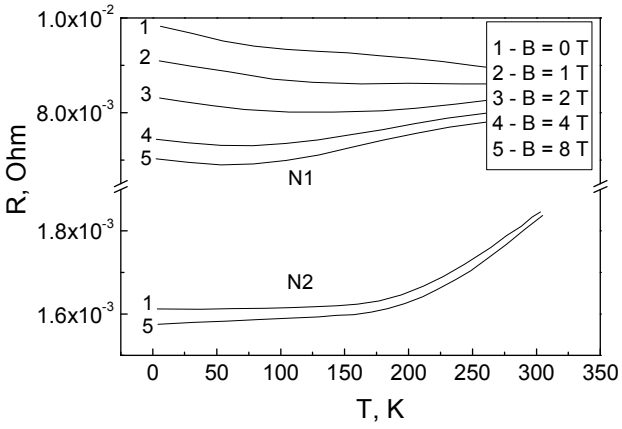

Fig. 7. Temperature dependence of the resistivity of samples No.1 and No.2 measured in a magnetic field directed along the current flow.

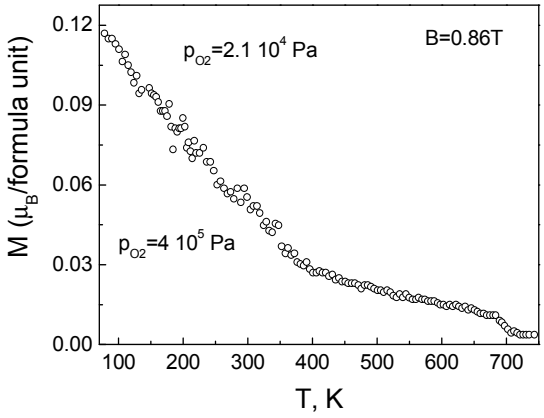

Fig. 8. Temperature dependence of the magnetization of SFMO samples annealed at 1173 K at different oxygen partial pressures.

Conclusions

The presented work has shown that $Sr_2FeMoO_{6\pm\delta}$ synthesis using partially reduced precursors of $SrFeO_{3-x}$ and $SrMoO_{4-y}$ comprising nanometer-sized grains, resulted in single phase $Sr_2FeMoO_{6\pm\delta}$ with superstructure ordering of Fe^{3+} and Mo^{5+} cations. Kinetic limitations were resolved in this ceramic charge by increasing the diffusivity of both of Fe^{3+} and Mo^{5+}. Crystallographic defects such as magnetic clusters and antisite defects Fe_{Mo} and Mo_{Fe}, for have large impact on magnetization and Curie temperature while the intergrain bonds determined the value of the magnetoresistance.

Acknowledgements

This work was supported by the German Research Foundation (DFG) as part of the Research Group FOR 520 and by Grant T08MC-043 of Belarusian Foundation for Basic Research.

References

[1] F.K. Patterson, C.W. Moeller and R. Ward: Inorg. Chem. 2 (1963), p. 196

[2] C.L. Yuan, S.G. Wang, W.H. Song, T. Yu, J.M. Dai, S.L. Ye and Y.P. Sun: Appl. Phys. Lett. 75 (1999), p. 3853

[3] K.I. Kobayashi, T. Kimura, H. Sawada, K. Terakura and Y. Tokura: Nature 395 (1998), p. 677

[4] D. Sánchez, J.A. Alonso, M. García-Hernández, M.J. Martínez-Lope, J.L. Martínez and A. Mellergard: Phys. Rev. B 65 (2002), p. 104426

[5] O. Chmaissem, R. Kruk, B. Dabrowski, D.E. Brown, X. Xiong, S. Kolesnik, J.D. Jorgensen and C.W. Kimbal: Phys. Rev. B 62 (2000), p. 14197

[6] M.K. Chung, P.J. Huang, W.-H. Li, C.C. Yang, T.S. Chan, R.S. Liu, S.Y. Wu and J.W. Lynn: Physica B 385-386 (2006), p. 418

[7] D.D. Sarma, P. Mahadevan, T. Saha-Dasgupta, S. Ray and A. Kumar: Phys. Rev. Lett. 85 (2000), p. 2549

[8] M. Itoh, I. Ohta and Y. Inaguma: Mater. Sci. Eng. B 41 (1996), p. 55

[9] Y. Tomioka, T. Okuda, Y. Okimoto, R. Kumai, K.-I. Kobayashi and Y. Tokura: Phys. Rev. B 61 (2000), p. 422

[10] L.l. Balcells, J. Navarro, M. Bibes, A. Roig, B. Martínez and J. Fontcuberta: Appl. Phys. Lett. 78 (2001), p. 781

[11] J. Rager, M. Zipperle, A. Sharma and J.L. MacManus-Driscoll: J. Am. Ceram. Soc. 87 (2004), p. 1330

[12] T.-T. Fang, M.S. Wu and T.F. Ko: J. Mat. Sci. Lett. 20 (2001), p. 1609

[13] A.S. Ogale, S.B. Ogale, R. Ramesh and T. Venkatessan: Appl. Phys. Lett. 75 (1999), p. 537

[14] Y. Takeda, K. Kanno, T. Takada, O. Yamamoto, M. Takano, N. Nakayama and Y. Bando: J. Solid State Chem. 63 (1986), p. 237

[15] M. Watahiki, J. Suzuki, Y. Tomioka and Y. Tokura: J. Phys. Soc. Jpn. 70 Suppl.A (2001), p. 67